

Eguchi, Kei; Kozono, Yutaka; Ishibashi, Takaaki; Asadi, Farzin

Article

Design of a dual-input cross-connected charge pump utilizing scavenged energy

Energy Reports

Provided in Cooperation with:

Elsevier

Suggested Citation: Eguchi, Kei; Kozono, Yutaka; Ishibashi, Takaaki; Asadi, Farzin (2020) : Design of a dual-input cross-connected charge pump utilizing scavenged energy, Energy Reports, ISSN 2352-4847, Elsevier, Amsterdam, Vol. 6, Iss. 2, pp. 228-234, <https://doi.org/10.1016/j.egy.2019.11.067>

This Version is available at:

<https://hdl.handle.net/10419/243883>

Standard-Nutzungsbedingungen:

Die Dokumente auf EconStor dürfen zu eigenen wissenschaftlichen Zwecken und zum Privatgebrauch gespeichert und kopiert werden.

Sie dürfen die Dokumente nicht für öffentliche oder kommerzielle Zwecke vervielfältigen, öffentlich ausstellen, öffentlich zugänglich machen, vertreiben oder anderweitig nutzen.

Sofern die Verfasser die Dokumente unter Open-Content-Lizenzen (insbesondere CC-Lizenzen) zur Verfügung gestellt haben sollten, gelten abweichend von diesen Nutzungsbedingungen die in der dort genannten Lizenz gewährten Nutzungsrechte.

Terms of use:

Documents in EconStor may be saved and copied for your personal and scholarly purposes.

You are not to copy documents for public or commercial purposes, to exhibit the documents publicly, to make them publicly available on the internet, or to distribute or otherwise use the documents in public.

If the documents have been made available under an Open Content Licence (especially Creative Commons Licences), you may exercise further usage rights as specified in the indicated licence.



<https://creativecommons.org/licenses/by-nc-nd/4.0/>

The 6th International Conference on Power and Energy Systems Engineering (CPESE 2019),
September 20–23, 2019, Okinawa, Japan

Design of a dual-input cross-connected charge pump utilizing scavenged energy

Kei Eguchi^{a,*}, Yutaka Kozono^a, Takaaki Ishibashi^b, Farzin Asadi^c

^a Department of Information Electronics, Fukuoka Institute of Technology, 3-30-1 Wajirohigashi, Higashi-ku, Fukuoka, 811-0295, Japan

^b Department of Electronics Engineering and Computer Science, National Institute of Technology, Kumamoto College, 2659-2 Suya, Koshi-shi, Kumamoto, 861-1102, Japan

^c Mechatronics Engineering Department, Kocaeli University, Umuttepe Yerleşkesi 41380, Kocaeli, Turkey

Received 2 October 2019; accepted 22 November 2019

Abstract

This paper presents a novel dual-input cross-connected charge pump utilizing scavenged energy. The proposed converter has two input sources: a battery input and a scavenged energy input. Unlike existing charge pumps, the proposed converter alleviates the energy consumed in a battery source by utilizing the scavenged energy. Therefore, the proposed converter can extend the lifetime of a battery source. Furthermore, the cross-connected structure offers not only higher voltage gain but also faster response speed than existing charge pumps. Through theoretical analysis and simulation program with integrated circuit emphasis (SPICE) simulation, the proposed converter demonstrates high power efficiency and high output voltage, where the proposed converter is compared with series-parallel converter, traditional charge pump, and Fibonacci converter. Concretely, about 90% power efficiency can be achieved by the proposed converter when the output power is 15 μ W, and the settling time is less than 19 μ s when the output load is 500 k Ω . Furthermore, the feasibility of the proposed converter is confirmed by breadboard experiments, where the experimental circuit is built with commercially available ICs.

© 2019 Published by Elsevier Ltd. This is an open access article under the CC BY-NC-ND license (<http://creativecommons.org/licenses/by-nc-nd/4.0/>).

Peer-review under responsibility of the scientific committee of the 6th International Conference on Power and Energy Systems Engineering (CPESE 2019).

Keywords: Energy harvesting; Dual inputs; Inductor-less converters; Cross-connected structure; Charge pump

1. Introduction

Recently, energy harvesting [1,2] is one solution to save energy in electric appliances, because some of wasted energy are captured by energy harvesting collectors and are used for electric appliances. In the energy harvesting collectors, ambient energy is converted into electrical energy. However, the application field of energy harvesting systems is limited, because typical power densities provided by energy harvesting collectors is very low such as μ W/cm³–mW/cm³. Therefore, power converters, namely, DC/DC [3,4], AC/DC [5], AC/AC [6], and DC/AC [7,8],

* Corresponding author.

E-mail address: eguti@fit.ac.jp (K. Eguchi).

<https://doi.org/10.1016/j.egy.2019.11.067>

2352-4847/© 2019 Published by Elsevier Ltd. This is an open access article under the CC BY-NC-ND license (<http://creativecommons.org/licenses/by-nc-nd/4.0/>).

Peer-review under responsibility of the scientific committee of the 6th International Conference on Power and Energy Systems Engineering (CPESE 2019).

are an essential component for the design of efficient energy harvesting systems. Among others, an inductor-less dc–dc converter is a suitable solution to realize efficient energy harvesting systems, because it can provide low electromagnetic interference (EMI) noise, small size, light weight, and so on. In these last few decades, researchers have proposed many kinds of inductor-less dc–dc converters. For example, series–parallel type converter [7], charge pump [2,4], Fibonacci converter [8,9], and so on. However, these existing converters suffer from the lack of harvested energy, because electrical energy scavenged by energy harvesting collectors is very small. Furthermore, most of them require a big output capacitor to suppress ripple noise, because an output voltage is provided only in a half clock cycle.

In this paper, we propose a dual-input cross-connected charge pump utilizing scavenged energy. Unlike existing techniques, we utilize the harvested energy as assistance to a battery input. Therefore, the proposed converter can extend the lifetime of a battery source, where the energy consumption of a battery source is alleviated by utilizing the scavenged energy. Furthermore, high voltage gain and small ripple can be achieved by the cross-connected structure [1,9]. To demonstrate the effectiveness of the proposed converter with $6\times$ step-up gain, the performance of the proposed converter is compared with that of existing converters, namely, series–parallel converter [7], traditional charge pump [2,4], and Fibonacci converter [8,9], by using simulation program with integrated circuit emphasis (SPICE) simulations and theoretical analysis.

This paper consists of 6 parts. First, the circuit configuration of the proposed converter is explained in Section 2. Next, the characteristics of the proposed converter is clarified theoretically in Section 3. Then, in Section 4, the performance evaluation is performed by comparing the proposed converter with the existing converters [2,6–9]. After that, in order to confirm the feasibility of the proposed converter, breadboard experiments are conducted in Section 5. Finally, the result of this work is summarized in Section 6.

2. Circuit configuration

Fig. 1 illustrates an example of the circuit configuration of the proposed dual-input cross-connected charge pump. Unlike existing converters, the proposed converter has two-input sources: a battery input V_{in1} and a scavenged energy input V_{in2} . By driving switches S_1 and S_2 by two-phase clock pulses, the output voltage is given by

$$V_{out} = 3(V_{in1} + V_{in2}). \tag{1}$$

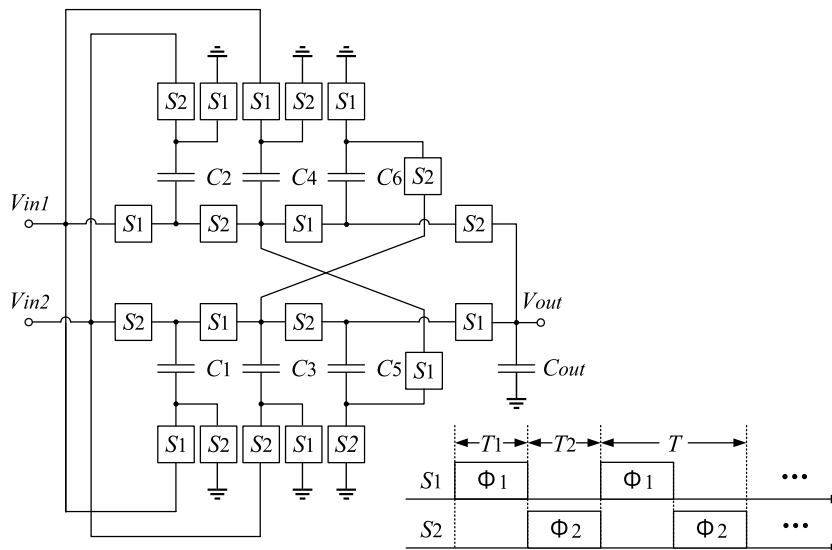


Fig. 1. Circuit configuration of the proposed dual-input cross-connected charge pump with $6\times$ step-up gain.

As Eq. (1) shows, the output voltage of the proposed converter is expressed by combining V_{in1} and V_{in2} . Therefore, the proposed converter can alleviate the energy consumed in a battery source. Concretely, if $V_{in1} = V_{in2}$, the energy consumption in a battery source becomes half, because the proposed converter has a symmetrical topology.

3. Theoretical analysis

In the theoretical analysis, the equivalent circuit is obtained by using the instantaneous equivalent circuit shown in Fig. 2, where the equivalent circuit is expressed by the six-terminal equivalent model shown in Fig. 3 [4]. In Fig. 3, m_1 and m_2 are the turn ratios of an ideal transformer, RSC is the internal resistance of the power converter, and R_L is the output load. The theoretical analysis is simplified by assuming the conditions that 1. Parasitic elements are small, 2. Time constant is much larger the period of clock pulses, and 3. Two transformers do not resonate each other. Using Fig. 3, we can derive the characteristics of the proposed converter, namely, output voltage and power efficiency [10].

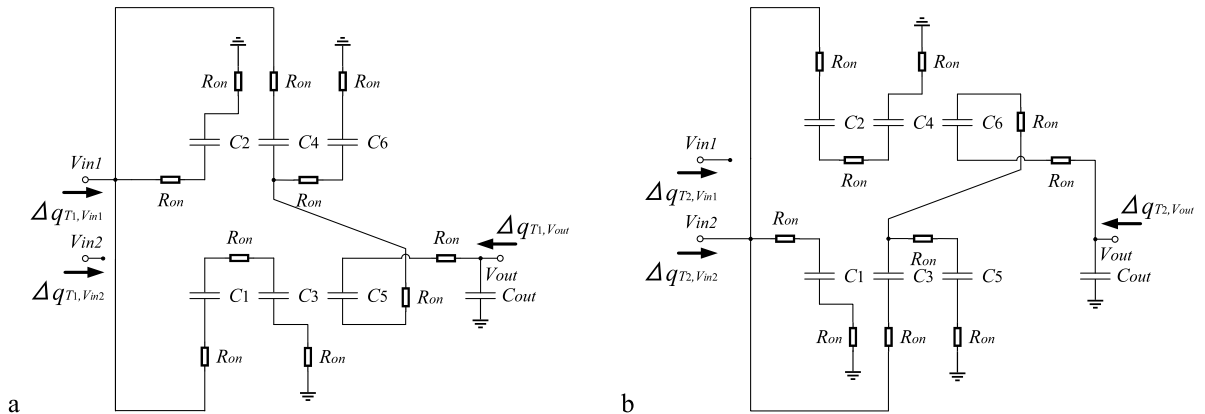


Fig. 2. Instantaneous equivalent circuits: (a) state- T_1 ; (b) state- T_2 .

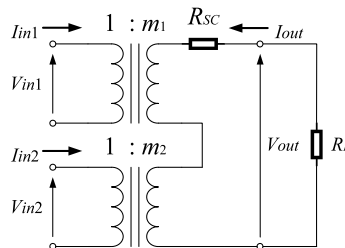


Fig. 3. Six-terminal equivalent model.

First, in order to obtain the relation between the inputs and the output, the differential value of electric charges $\Delta q_{T_i}^k$ in C_k ($k = 1, \dots, 6$) is discussed by using Fig. 2, where R_{on} is the on-resistance of S_i ($i = 1, 2$), $\Delta q_{T_i, v_{in1}}$ and $\Delta q_{T_i, v_{in2}}$ are the electric charge of the V_{in1} and V_{in2} in State- T_i , and $\Delta q_{T_i, v_{out}}$ ($i = 1, 2$) is the electric charge of the output terminal in State- T_i . In a steady state, the electric charges of C_k are the same at the start and end of the cycle T , because the overall change in electric charges is zero. Thus, the differential value $\Delta q_{T_i}^k$ satisfies

$$\Delta q_{T_1}^k + \Delta q_{T_2}^k = 0. \quad (2)$$

In Eq. (2), the interval of T_1 and T_2 satisfies $T = T_1 + T_2$ and $T_1 = T_2 = T/2$, where T is a period of clock pulses. By using Kirchhoff's current law, the relation between $\Delta q_{T_i}^k$'s is obtained by

$$\Delta q_{T_1, v_{in1}} = -\Delta q_{T_1}^1 + \Delta q_{T_1}^2 - \Delta q_{T_1}^4, \quad \text{and} \quad \Delta q_{T_2, v_{in1}} = 0, \quad (3)$$

$$\Delta q_{T_1, v_{in2}} = 0, \quad \text{and} \quad \Delta q_{T_2, v_{in2}} = \Delta q_{T_2}^1 - \Delta q_{T_2}^2 - \Delta q_{T_2}^3, \quad (4)$$

$$\Delta q_{T_1, v_{out}} = \Delta q_{T_1}^{out} + \Delta q_{T_1}^5, \quad \text{and} \quad \Delta q_{T_2, v_{out}} = \Delta q_{T_2}^{out} + \Delta q_{T_2}^6, \quad (5)$$

$$\Delta q_{T_2}^6, \Delta q_{T_1}^1 = -\Delta q_{T_1}^3, \quad \Delta q_{T_1}^5 = \Delta q_{T_1}^4 + \Delta q_{T_1}^6, \quad (6)$$

$$\Delta q_{T_2}^2 = -\Delta q_{T_2}^4, \quad \text{and} \quad \Delta q_{T_2}^6 = \Delta q_{T_2}^3 + \Delta q_{T_2}^5, \quad (6)$$

Using Eqs. (2)–(6), we have the average inputs/output currents, I_{in1} , I_{in2} , and I_{out} , as follows:

$$\begin{aligned}
 I_{in1} &= \frac{\Delta q_{v_{in1}}}{T} = \frac{\Delta q_{T_1, v_{in1}} + \Delta q_{T_2, v_{in1}}}{T}, \\
 I_{in2} &= \frac{\Delta q_{v_{in2}}}{T} = \frac{\Delta q_{T_1, v_{in2}} + \Delta q_{T_2, v_{in2}}}{T}, \\
 \text{and } I_{out} &= \frac{\Delta q_{v_{out}}}{T} = \frac{\Delta q_{T_1, v_{out}} + \Delta q_{T_2, v_{out}}}{T},
 \end{aligned}
 \tag{7}$$

because the overall change in the electric charges, $\Delta q_{T_i, v_{in}}$, $\Delta q_{T_i, v_{in}}$, and $\Delta q_{T_i, v_{out}}$, is zero in the steady state. By substituting Eqs. (2)–(6) into Eq. (7), we obtain the relation between the inputs and the output as follows:

$$I_{in1} = -3I_{out}, \quad I_{in2} = -3I_{out}, \quad \text{and} \quad m_1 = m_2 = 3
 \tag{8}$$

Next, the total consumed energy, W_T , of Fig. 2 is discussed to derive R_{SC} . As Fig. 2 shows, the consumed energy of Fig. 2(a) is equal to that of Fig. 2(b), because the proposed converter has a symmetrical topology. Therefore, we can express W_T as follows:

$$\begin{aligned}
 W_T &= 2 \times \left\{ 3R_{on} \frac{(\Delta q_{T_1}^3)^2}{T_1} + 2R_{on} \frac{(\Delta q_{T_1}^2)^2}{T_1} + 2R_{on} \frac{(\Delta q_{T_1}^5)^2}{T_1} + 2R_{on} \frac{(\Delta q_{T_1}^6)^2}{T_1} + R_{on} \frac{(\Delta q_{T_1}^4)^2}{T_1} \right\} \\
 &= 28R_{on} \frac{(\Delta q_{v_{out}})^2}{T}.
 \end{aligned}
 \tag{9}$$

From Eq. (9), we get R_{SC} as $28R_{on}$, because W_T of Fig. 3 can be expressed as

$$W_T \triangleq \left(\frac{q_{v_{out}}}{T} \right)^2 R_{SC} T.
 \tag{10}$$

Finally, we obtain the equivalent circuit of the proposed converter as shown in Fig. 4. From Fig. 4, the output voltage and the power efficiency can be derived as

$$V_{out} = 3(V_{in1} + V_{in2}) \left\{ \frac{R_L}{R_L + 28R_{on}} \right\} \quad \text{and} \quad \eta = \frac{R_L}{R_L + 28R_{on}}.
 \tag{11}$$

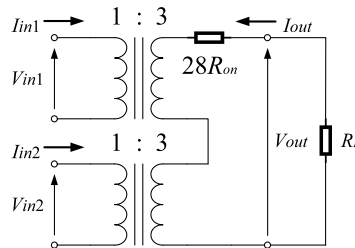


Fig. 4. Equivalent circuit of the proposed converter.

As Eq. (11) shows, the internal resistance $R_{SC} (= 28R_{on})$ is the important factor to achieve high power efficiency [11].

4. Performance evaluation

In this section, we conducted SPICE simulations in order to justify the effectiveness of the proposed converter. To compare the performance of the proposed converter with that of existing converters, the SPICE simulations were performed under the conditions that $V_{in1} = V_{in2} = 0.3$ V, $R_{on} = 1$ Ω , $f = 1$ MHz, and $C_1 = \dots = C_6 = C_{out} = 200$ pF. In the SPICE simulations, the proposed converter was compared with the existing converters, namely, series–parallel type converter [7], traditional charge pump [2,4], and Fibonacci converter [8,9].

Fig. 5 demonstrates the comparison result concerning power efficiency. As Fig. 5 shows, the power efficiency of the proposed converter is the highest when the output power is more than 13 μ W. Concretely, the proposed converter can achieve about 90% power efficiency when the output power is 15 μ W. Fig. 6 depicts the comparison result in

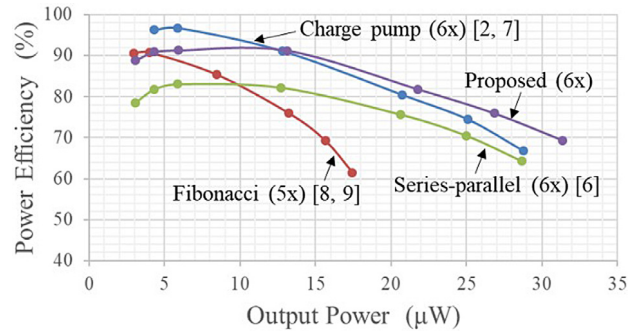


Fig. 5. Simulated power efficiency.

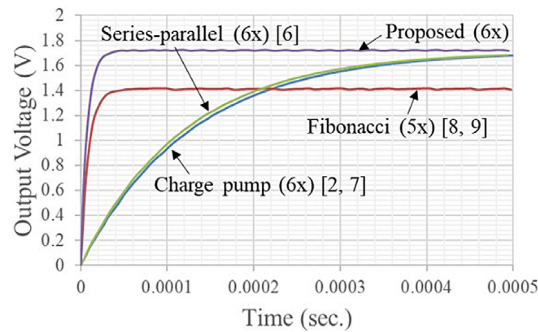


Fig. 6. Simulated transient characteristic.

transient characteristic, where the output load was set to 500 k Ω . As you can see from Fig. 6, the proposed converter is the fastest among them. Concretely, the settling time of the proposed converter is less than 19 μ s. Table 1 shows the number of circuit components. As Table 1 shows, unlike existing converters, the proposed converter can offer an output voltage in all cycles, although the number of circuit components for the proposed converter is slightly bigger than that for the existing converters. In other words, the proposed converter can achieve smaller ripple noise than the existing converters. Furthermore, owing to the dual-input topology, the proposed converter can extend the lifetime of a battery source.

Table 1. Number of circuit components.

Topology	Gain	Input type	Output cycle	Number of switches	Number of capacitors
Proposed converter	6 \times	Dual	Full cycle	20	7
Series–parallel type converter	6 \times	Single	Half cycle	16	6
Traditional charge pump	6 \times	Single	Half cycle	17	6
Fibonacci converter	5 \times	Single	Half cycle	10	4

5. Experiments

In this section, the feasibility of the proposed dual-input topology is confirmed by breadboard experiments. In this experiment, the proposed converter was built with commercially available ICs, namely, photo MOS relays AQV 212, darlington sink drivers TD62004APG, a microcontroller PIC, and electrolytic capacitors. Fig. 7 demonstrates the measured output voltage when V_{in1} is about 0.3 V and V_{in2} is about 0.28 V, where the ideal output voltage of the experimental circuit is 1.74 V. As Fig. 7 shows, the measured output voltage is 1.63 V at the output load 510 k Ω . In Fig. 7, the voltage efficiency of the experimental circuit is about 93.7%, because the ideal output voltage is 1.74 V. Fig. 8 demonstrates the measured output voltage when V_{in1} is about 0.39 V and V_{in2} is about 0.19 V, where the ideal output voltage of the experimental circuit is 1.74 V. As Fig. 8 shows, the measured output voltage

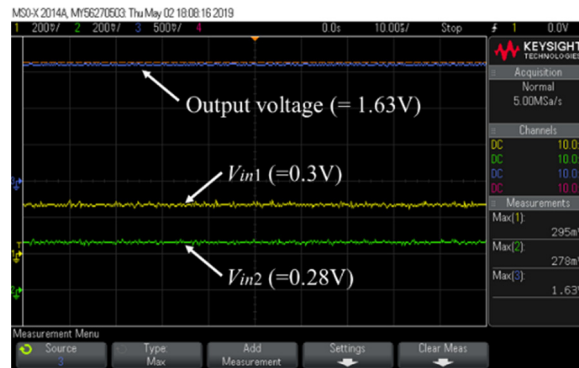


Fig. 7. Measured output voltage ($V_{in1} = 0.3$ V and $V_{in2} = 0.3$ V).

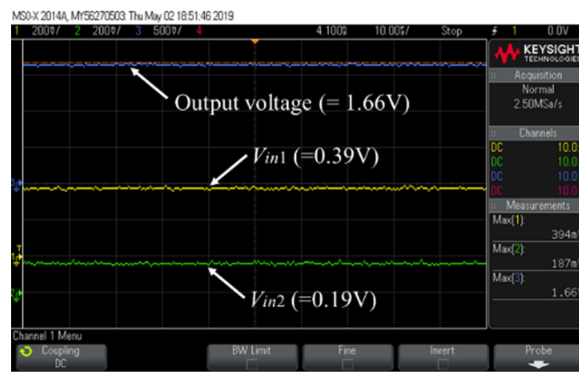


Fig. 8. Measured output voltage ($V_{in1} = 0.4$ V and $V_{in2} = 0.2$ V).

is 1.66 V at the output load 510 k Ω . In Fig. 8, the voltage efficiency of the experimental circuit is about 95.4%, because the ideal output voltage is 1.74 V. From Figs. 7 and 8, the feasibility of the proposed converter can be confirmed.

6. Conclusion

A novel dual-input cross-connected charge pump has been proposed in this paper. To alleviate the energy consumed in a battery source, the proposed converter provides a stepped-up voltage by utilizing scavenged energy. Therefore, the proposed converter can extend the lifetime of a battery source. The characteristics of the proposed converter was investigated by theoretical analysis, SPICE simulations, and bread board experiments. The performance evaluation demonstrated that 1. The proposed converter can achieve higher power efficiency than the existing converters, namely, series–parallel type converter, traditional charge pump, and Fibonacci converter. When the output power was 15 μ W, the power efficiency of the proposed converter was about 90%, 2. The proposed converter was the faster than the existing converters. When the output load was 500 k Ω , the settling time of the proposed converter was less than 19 μ s, and 3. The feasibility of the proposed converter was confirmed through experiments. The experimental circuit achieved high step-up gain.

The future enhancement of this work is to integrate the proposed converter into an IC chip and justify the effectiveness of the proposed converter experimentally.

References

- [1] Do Wanlok, Fujisaki Haruka, Asadi Farzin, Eguchi Kei. A cross-connected charge pump for energy harvesting applications. *Int J Innovative Comput Inf Control* 2019;15(3):2335–42.
- [2] Wang Yu, Yan Na, Min Hao, Shi C-J Richard. A high-efficiency split-merge charge pump for solar energy harvesting. *IEEE Trans Circuits Syst II: Express Briefs* 2017;64(5):545–9.

- [3] Tulasi P Narasimha, Aithepalli D Lakshmi. Droop control of bi-directional dc-dc converter for improved voltage regulation and load sharing in dc microgrid. *Int J Intell Eng Syst* 2019;12(3):228–43.
- [4] Eguchi Kei, Fujimoto Kuniaki, Sasaki Hirofumi. A hybrid input charge-pump using micropower thermoelectric generators. *IEEJ Trans Electr Electron Eng* 2012;7(4):415–22.
- [5] Abe Kanji, Smerpitak Krit, Pongswatd Sawai, Oota Ichirou, Eguchi Kei. A step-down switched-capacitor ac-dc converter with double conversion topology. *Int J Innovative Comput Inf Control* 2017;13(1):319–30.
- [6] Eguchi Kei, Do Wanglok, Kittipanyangam Soranut, Abe Kanji, Oota Ichirou. Design of a three-phase switched-capacitor ac-ac converter with symmetrical topology. *Int J Innovative Comput Inf Control* 2016;12(5):1411–21.
- [7] Oota Manami, Terada Shinya, Eguchi Kei, Oota Ichirou. Development of switched-capacitor bi-directional dc-ac converter for inductive and capacitive loads. In: *Proc. 2009 IEEE international symposium on industrial electronics*. 2009, p. 1618–23.
- [8] Abe Kanji, Do Wanglok, Kittipanyangam Soranut, Oota Ichirou, Eguchi Kei. A Fibonacci-type dc-ac inverter designed by switched capacitor technology. *Int J Innovative Comput Inf Control* 2016;12(4):1197–207.
- [9] Eguchi Kei, Pongswatd Sawai, Asadi Farzin, Fujisaki Haruka. A high voltage gain SC DC-DC converter based on cross-connected Fibonacci-type converter. In: *Proc. of 2018 international conference on engineering, applied sciences, and technology*. 2018. <http://dx.doi.org/10.1109/ICEAST.2018.8434465>.
- [10] Eguchi Kei, Oota Ichirou, Terada Shinya, Inoue Takahiro. A design method of switched-capacitor power converters by employing a ring-type power converter. *Int J Innovative Comput Inf Control* 2009;5(10A):2927–38.
- [11] Eguchi Kei, Pongswatd Sawai, Tirasesth Kitti, Sasaki Hirofumi, Inoue Takahiro. Optimal design of a single-input parallel dc-dc converter designed by switched capacitor techniques. *Int J Innovative Comput Inf Control* 2010;6(1):215–27.